

Characterization of Hydrogenated Graphene on Copper

Research Thesis

Presented in Partial Fulfillment of the Requirements for graduation

“with Research Distinction in Physics” in the undergraduate colleges of
The Ohio State University

By
Kara Mattioli

The Ohio State University
April 2015

Project Advisor: Professor Jay Gupta, Department of Physics

Characterization of Hydrogenated Graphene on Copper

- I. Abstract
- II. Introduction
 - A. Graphene and its Fascinating Properties
 - B. CVD Graphene Growth and Graphene Transfer with PMMA
 - C. Hydrogenated Graphene and its Advantages over Non-Functionalized Graphene
 - D. Spectral Characterization Techniques
 - 1. Raman Spectroscopy
 - 2. X-ray Photoelectron Spectroscopy
- III. Experimental Methods
 - A. Procedure for Hydrogenating Graphene in Vacuum with Molecular Hydrogen
 - B. X-ray Photoelectron Spectroscopy
 - C. Raman Spectroscopy
- IV. Results and Discussion
 - A. Substrate Dependence of Hydrogenation
 - B. Effect of Intercalated Oxygen on Hydrogenation
- V. Conclusion
- VI. Acknowledgements
- VII. References

I. Abstract

Graphene is a recently discovered material comprised of a single layer of carbon atoms arranged in a hexagonal lattice structure. The incredible thickness of graphene, only a single layer of atoms, has resulted in it being termed a “2D” material and also gives rise to promising electronic and optical properties. However, potential uses of graphene are limited without a way to control its properties and vary them for different applications.

One way to modify the electronic properties of graphene is to hydrogenate it, which chemically bonds a layer of hydrogen atoms to its surface¹. When graphene is hydrogenated, it has insulating instead of semimetallic properties due to the creation of a band gap in graphene’s density of states². Changing the size of a band gap determines how insulating a material will be. The ability to fine-tune electronic properties of 2D materials is a major area of current research due to its implications for future electronic devices.

Several methods exist for hydrogenating graphene, but some risk damaging the graphene and its remarkable properties. In this study, a method to hydrogenate graphene in vacuum is tested, which would be an easier method of hydrogenation and a convenient way to prepare hydrogenated graphene for further experiments in vacuum. Graphene hydrogenation was first attempted on silicon dioxide, the substrate onto which graphene is most commonly transferred after it is grown on copper. However, at the hydrogenation temperatures used in this method, chemical residue left on the graphene from the transfer process formed amorphous carbon on the graphene surface and severely distorted the graphene structure.

The new method to hydrogenate graphene on copper in vacuum is tested to determine if graphene can be hydrogenated by heating it in vacuum and exposing it to molecular hydrogen.

Raman spectroscopy and X-ray photoelectron spectroscopy are used to determine whether the hydrogenations are successful. Since there are no transfer residues on graphene after it is grown on copper, this procedure prevents the formation of amorphous carbon on the graphene surface. Raman spectroscopy is a widely used method to study graphene and provides information as to how its lattice vibrations are affected by defects and chemical bonding of atoms on its surface. X-ray photoelectron spectroscopy (XPS) gives information about the chemical bonds that are present in a material. XPS determines whether a significant amount of carbon-hydrogen bonds are present compared to the carbon-carbon bonds that are already present in graphene.

Hydrogenated graphene could be used for a broader range of experiments if it could be produced more easily and efficiently. Finding a new method of creating this novel material and optimizing its quality would further the study of its potential uses in technology as well as the current knowledge of 2D materials.

II. Introduction

A. Graphene and its Fascinating Properties

Graphene is a single layer of carbon atoms arranged in a hexagonal lattice structure. For such a seemingly insignificant layer of atoms that are bonded together, it has attracted an overwhelming amount of interest from the scientific and engineering communities. Its high mobility, incredible strength, and nearly pure transparency, among other properties^{3,4}, prompt many to claim that graphene has the potential to replace silicon in electronic devices. Its electron transport, which is governed by the Dirac equation, provides those interested in quantum electrodynamics access to a realistically scalable system for experimentation and study⁵. As the first material to usher in the wave of interest with 2D materials, graphene continues to fascinate researchers with its properties that are still being studied and expounded on every day.

B. CVD Graphene Growth and Graphene Transfer with PMMA

Significant research has focused on creating a method to grow high-quality graphene that could eventually be scaled up to industry production requirements. One method that shows promising results for potential industry application is graphene growth by chemical vapor deposition (CVD). While there are many variations of the CVD method, most involve heating a copper substrate in vacuum near its melting point while flowing a hydrocarbon gas over the substrate⁶. The copper substrate catalyzes the decomposition of the hydrocarbon to form graphene⁷. The graphene samples in this study were grown on copper by CVD using methane as a hydrocarbon precursor. After graphene growth on copper, graphene is transferred from copper to a silicon wafer with 300nm silicon dioxide (Si/SiO₂). Most transfer processes involve the use of polymethyl methacrylate, abbreviated PMMA, which is a polymer commonly used to stabilize the single atomic layer of graphene during transfer from copper to Si/SiO₂⁸.

C. Hydrogenated Graphene and its Advantages over Non-Functionalized Graphene

While graphene has many properties that can be used in industrial applications, its properties are limited without a way to control or modify them. Functionalizing graphene by covalently bonding another element to its surface is one way of changing its electronic properties, and has already been accomplished with oxygen, fluorine, and hydrogen¹. Creating hydrogenated graphene is of special interest because it could potentially be used to create hydrogen storage systems⁹. In addition, hydrogenation causes graphene's electrical properties to become more insulating². Fully hydrogenated graphene, graphane, is predicted to have a bandgap of 3.5 eV^{9,10}. Partial hydrogenation allows for fine tuning of graphene's electrical properties, as the extent to which the graphene is hydrogenated determines whether it has

magnetic, metallic, or semiconducting properties¹⁰.

The most common method of graphene hydrogenation is briefly exposing graphene to an atomic hydrogen plasma treatment^{1,2}. The motivation for attempting to hydrogenate graphene by annealing it and exposing it to molecular hydrogen is due to the fact that a similar procedure successfully hydrogenated diamond¹¹.

D. Spectral Characterization Techniques

1. Raman Spectroscopy

Raman spectroscopy is a technique in which a laser is used to excite atoms in a sample into vibrationally excited states. In a solid, a photon from the laser excites an electron-hole pair³. As this electron-hole pair decays back down to a more stable energy state, a phonon is created and another photon is emitted³. The Raman spectrometer measures the difference in energy between the initial photon, whose energy was equal to the energy of the laser, and the re-emitted photon. This difference is called the Raman shift.

The Raman spectrum of graphene has been extensively studied and is characterized by three distinct peaks: the D peak, G peak, and 2D peak³. The wavenumbers at which these peaks occur give information about the phonon modes of graphene; each peak represents a different vibrational mode of the atoms in the graphene lattice³. The D peak is only activated when defects are present in the graphene, and is therefore used as a measure of disorder in a graphene sample. However, the D peak is also observed to appear when graphene is hydrogenated; the change in hybridization that occurs when graphene is hydrogenated registers as a significant defect in the graphene Raman spectrum². The G and 2D peaks in graphene are always present because no defects are required for their activation.³

2. X-ray Photoelectron Spectroscopy

X-ray photoelectron spectroscopy, abbreviated as XPS, is a technique in which a sample is bombarded with x-rays that eject electrons in the sample from their energy orbitals¹². For an electron to be ejected from an atom, it must have an energy greater than the binding energy of that electron to the atom. For any energy less than the binding energy, the Coulomb attraction between the electron and the nucleus of the atom will be too strong for the electron to escape from the atom. X-rays can transfer enough energy to electrons so that they can not only overcome the binding energy minimum requirement of exiting the atom, but they can also exit the atom with some kinetic energy as well.

The basic idea of XPS is to use energy conservation laws to determine the binding energies of compounds in a sample, and binding energies provide a wonderful clue to chemically identify components of a sample¹². The energy of the initial x-ray source, which is known in XPS, must equal the kinetic energy of an ejected electron plus the binding energy of the atomic energy orbital from which it was ejected¹². Therefore, an x-ray photoelectron spectrometer can indirectly measure the binding energies of electrons in various compounds by directly measuring the kinetic energies the electrons have when they are ejected from the sample. One more factor must be included in the simple energy conservation equation: the work function of the sample. For a solid, the work function is the difference in energy between the vacuum level and the Fermi level of a sample¹². In the x-ray photoelectron spectrometer, the sample and the spectrometer are in electrical contact and their work functions are identical¹². Therefore only the work function of the spectrometer must be known to calculate the binding energies. The general equation used to calculate binding energies measured with XPS is the following¹²:

$$BE = h\nu - KE - \varphi_{spec}$$

where BE is the binding energy of the electron in a particular atom or compound, $h\nu$ is the initial energy of the x-ray, KE is the measured kinetic energy of the ejected electron, and φ_{spec} is the spectrometer work function. The binding energies are referenced to the Fermi level of the spectrometer and not to the vacuum level.

III. Experimental Methods

A. Procedure for Hydrogenating Graphene in Vacuum with Molecular Hydrogen

The graphene samples used in this study were CVD-grown on copper foils by the Graphene Factory, an undergraduate research group in the Department of Physics at The Ohio State University. Graphene samples are first placed on a home-built UHV compatible sample heater. The heater is placed in vacuum and pumped down to better than 10^{-6} mbar. The vacuum pressure is monitored with an ion gauge.

The heater has a tantalum foil resistive element with two thin leads that are in electrical contact with electrical leads. The electrical leads extend through the flange so that they can be connected to an ex-situ power source. The middle of the tantalum foil is thicker than the leads and is cut into a serpentine pattern to maximize the heat dissipated through the filament. The tantalum foil is epoxied to a thin piece of alumina. The tantalum foil and alumina rest on top of a piece of bisque alumina. The sample is placed on top of the thin piece of alumina that is epoxied to the tantalum filament.

To heat the sample, a voltage is applied across the leads of the tantalum filament using an ex-situ power supply. Power is radiated from the filament proportional to the resistance of the filament and is absorbed by the sample and bisque alumina directly above the filament. The

samples are heated and cooled at a rate of 0.25 Volts per minute. An ex-situ Luxtron pyrometer is used to estimate the temperature of the graphene/Cu sample in vacuum. As graphene is almost completely transparent, the emissivities of copper were used to calibrate the pyrometer. The pyrometer reading is highly sensitive to the spot on which the pyrometer is focused, and the current vacuum setup does not allow for detailed positioning of the pyrometer to ensure that it is focused on the sample. As a result, the pyrometer reading is estimated to be accurate to within $\pm 100^{\circ}\text{C}$. To partially calibrate the pyrometer, a large graphene/Cu sample was used that almost completely covered the alumina of the heater beneath it. The pyrometer was scanned over the sample at a fixed voltage, and the temperature that was observed over the majority of the sample area was taken to be the temperature of the graphene/Cu sample.

The resistance of the tantalum filament does not change significantly over multiple heating cycles; therefore the voltage is used to systematically replicate heating at a given temperature. When the same voltage is applied across two separate samples, their resulting temperatures are assumed to be approximately equal. This assumption is implemented as a more accurate way of checking that the samples are heated to the same temperature, instead of solely using the pyrometer reading that is subject to significant error.

The graphene samples are heated to approximately $650\text{-}700^{\circ}\text{C}$ before molecular hydrogen is introduced into the chamber through a leak valve. Hydrogen is leaked in until the pressure in the chamber is greater by one order of magnitude. The temperature is held constant by keeping the voltage across the heater fixed while the samples are exposed to hydrogen for 30 minutes. After the hydrogen exposure, the hydrogen leak valve is immediately closed and the samples are cooled in vacuum. Samples are left in vacuum until they can be transferred to the x-ray photoelectron spectrometer vacuum chamber. Control samples are annealed at the same

temperatures as the hydrogenation samples for the same amount of time, but are not exposed to molecular hydrogen.

B. X-ray Photoelectron Spectroscopy (XPS)

X-ray photoelectron spectra are acquired with a Kratos Axis Ultra X-Ray Photoelectron Spectrometer. A monochromatic Aluminum source is used as the X-ray source. A Shirley background is used to subtract the background from the copper 2p, oxygen 1s, and carbon 1s data. All peaks are fit with Doniach-Sunjic lineshapes convoluted with Gaussian profiles. The asymmetry parameter used in the curve fits is 0.09.

C. Raman Spectroscopy

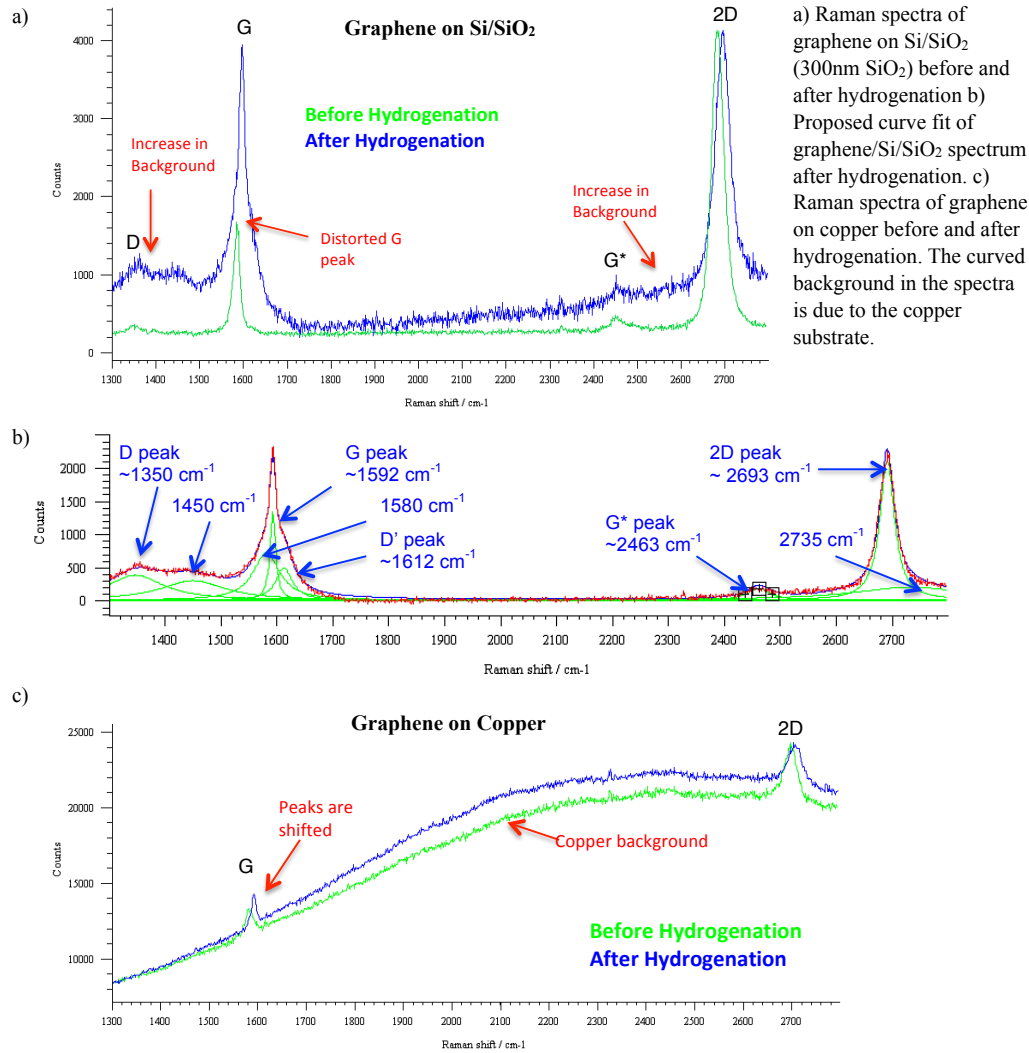
Raman spectra are acquired using a Renishaw InVia Raman Spectrometer with a 514nm laser. Spectra of graphene on Si/SiO₂ are acquired with a 20x objective and a 60 second exposure time. Spectra of graphene on copper are acquired with a 50x objective and an exposure time of 180 seconds. Spectra after hydrogenation and control procedures are acquired with a 50x objective, and exposure times of 180 and 210 seconds. Since the Raman laser spot size is approximately a micron in diameter, spectra are taken at several spots on the sample before and after the hydrogenation and control procedures to obtain an overall characterization of each sample. Power at the sample is less than 1 mW to avoid laser-induced heating of the sample. All peaks are fit with Lorentzian lineshapes.

IV. Results and Discussion

A. Substrate Dependence of Hydrogenation

Raman spectra of the graphene samples before and after hydrogenation reveal that the substrate onto which graphene is transferred significantly impacts whether the hydrogenation can be successful. Figure 1(a) displays Raman spectra before and after hydrogenation for graphene transferred onto Si/SiO₂. The pristine graphene spectrum before hydrogenation has few defects,

Figure 1: Raman Spectra Before and After Hydrogenation



as evidenced by a small signature in the spectrum at 1350 cm^{-1} , indicating the presence of a small D peak. After hydrogenation, the spectrum is radically deformed. A proposed curve fit shown in Figure 1(b) displays that the increased spectral background in the range of $1300\text{--}1700\text{ cm}^{-1}$ and $2200\text{--}2800\text{ cm}^{-1}$ is a result of the appearance of broad underlying peaks near the G and 2D graphene peaks¹³. The peaks at 1350 cm^{-1} , 1592 cm^{-1} , 2463 cm^{-1} , and 2693 cm^{-1} are attributed to intrinsic graphene peaks and correspond to the initial D, G, G*, and 2D peaks, respectively¹⁴. The peak at 1612 cm^{-1} is observed in severely defective graphene and is an additional graphene defect peak¹⁵. The peak at 1450 cm^{-1} is assigned to residual PMMA, and the peaks at 1580 cm^{-1} and 2735 cm^{-1} are assigned to amorphous carbon on the graphene surface^{13,16}. The severe distortion upon annealing graphene/Si/SiO₂ with residual PMMA supports the hypothesis that PMMA decomposes and forms amorphous carbon on the graphene surface. Amorphous and defective graphene is unlikely to form regions of hydrogenated graphene upon exposure to hydrogen, therefore the hydrogenation experiment was repeated with graphene on copper instead of graphene on Si/SiO₂.

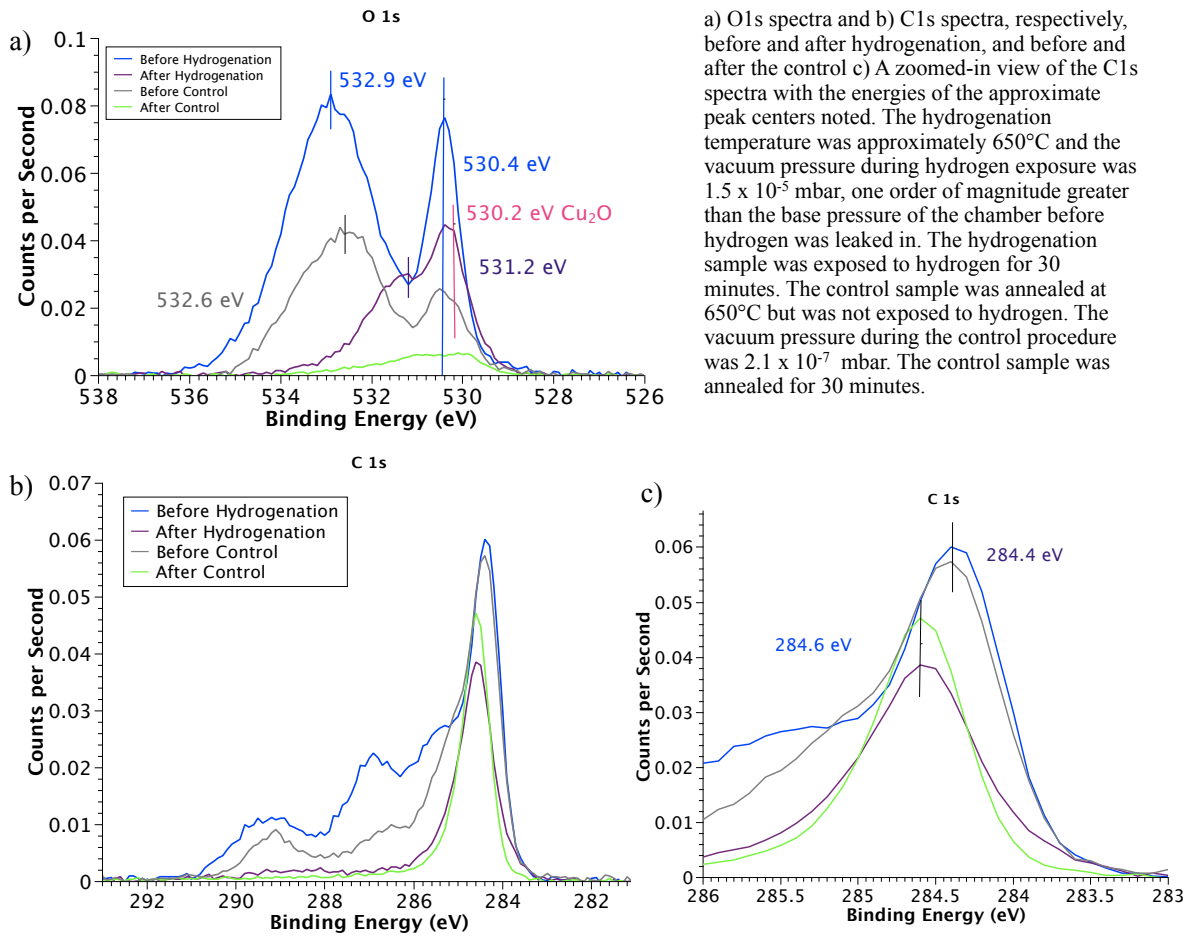
Compared to the effect of the hydrogenation on the graphene/Si/SiO₂ samples, the Raman spectra before and after the hydrogenation of graphene on copper show small changes. Figure 1(c) shows that the only main difference between the Raman spectra before and after graphene on copper is subjected to hydrogenation is that the G and 2D peaks are slightly shifted. Raman spectra of graphene on Si/SiO₂ have established that slight variations in the positions of the graphene peaks are due to intrinsic doping of the graphene¹⁷. It is therefore not unlikely that for graphene on copper, the Raman peaks may intrinsically vary in position by the same amount that they vary for graphene on Si/SiO₂. Variations in both peak lineshapes and positions were observed in spectra both before and after hydrogenation. Notably, the spectrum after

hydrogenation in Figure 1(c) does not display a sharp D peak at 1350 cm^{-1} , indicating that the sample is not hydrogenated². However, the post-hydrogenation spectrum also does not display any indications of damage to the graphene induced by annealing.

B. Effect of Intercalated Oxygen on Hydrogenation

The XPS spectra reveal that the hydrogenation process dramatically affects the oxygen and carbon content of the graphene/Cu sample. The XPS data observed before and after the graphene/Cu sample was exposed to hydrogenation, and before and after a different graphene/Cu sample was exposed to the control procedure are displayed in Figure 2. In the figure, all peaks

Figure 2: XPS Spectra of Graphene/Cu Before and After Hydrogenation



are normalized to the Cu $2p_{3/2}$ intensity at 932.6 eV. Both the hydrogenation and control samples

were subjected to annealing at approximately 650°C for 30 minutes; the only difference between the two samples is that the control sample was not exposed to hydrogen. Figure 2(b) shows that most of the satellite carbon peaks in the range of 286-291 eV are removed after hydrogenation and the control, and Figure 2(a) shows that two distinct oxygen peaks remain after hydrogenation that are not clearly observed after the control. One of these peaks, at 530.4 eV, has a shoulder at 530.2 eV, the accepted binding energy of Cu_2O ¹⁸. Cu_2O is known to form between CVD-grown graphene and copper due to oxygen intercalation after the graphene/Cu sample is removed from vacuum post-growth and exposed to air¹⁸. The presence of Cu_2O after hydrogenation suggests that a greater amount of intercalated oxygen remains between the graphene and the copper substrate after the hydrogenation than after the control.

The intercalated oxygen in CVD-grown graphene/Cu samples can be removed upon annealing the sample in vacuum¹⁸. The graphene/Cu samples that are subjected to hydrogenation are also annealed in vacuum, with the only exception that they are annealed in the presence of hydrogen. As seen in Figure 2(a), the presence of hydrogen during the annealing process preserves some of the Cu_2O that was initially present in the as-grown graphene/Cu sample. Before the hydrogenation, two peaks centered at 532.9 eV and 530.4 eV are present in the graphene/Cu sample. The peaks in the range of 531-536 eV are attributed to various oxygen-hydrogen and oxygen-carbon related bonds¹⁸, which are most likely due to adsorbed residue on the graphene/Cu surface. The 530.4 eV peak is attributed to a form of copper oxide, as it is very close in energy to the accepted Cu_2O binding energy of 530.2 eV, and has also been observed in studies of intercalated oxygen between graphene and copper¹⁸. After the hydrogenation, the peak centered at 532.9 eV disappears and is replaced with a peak centered at 531.2 eV, while the Cu_2O peak is still present. The 531.2 eV peak is attributed to an oxygen-hydrogen bond¹⁸. The

control sample displays a much weaker signal of residual copper oxide and oxygen-hydrogen bonds, but these compounds are clearly observed to remain on the sample after hydrogenation.

Now that the peaks in Figure 2(a) have been identified, it is imperative to form an understanding of why some of them disappear after the control procedure and why some of them are created or reappear after the hydrogenation procedure. Annealing in vacuum is known to get rid of organic residue on surfaces, and can sufficiently explain the removal of the 532.9 eV peak, which was assumed to be due to leftover residue on the graphene surface. The control sample also initially displays a peak corresponding to surface residue, centered at 532.6 eV, which is also removed after annealing. The residue peak on the control sample does not occur at the same binding energy as the residue peak on the hydrogenated spectrum, which is most likely due to the fact that the control sample and the hydrogenated sample were two different graphene/Cu growth samples. The fact that their spectral profiles are similar indicates that the same chemical residue is likely present on both samples, but in varying amounts. Since the binding energy is highly dependent on the local environment of oxygen atoms in the sample, variations in the amount and type of residue can shift the binding energy. The introduction of hydrogen into the vacuum chamber explains the appearance of the oxygen-hydrogen peak in the hydrogenated spectrum and accounts for why this peak does not appear in the control spectrum, where no hydrogen was introduced. The only peak whose existence has yet to be explained is the copper oxide peak, which is not removed by annealing in the case of hydrogen exposure.

The control sample was annealed for the same amount of time as the hydrogenation sample was annealed and exposed to hydrogen. Within 30 minutes at 650°C, the copper oxide is almost completely removed from the control sample while a significant amount still remains on the sample subjected to hydrogenation, which suggests that the hydrogen plays a role in

preserving the copper oxide between the graphene and the copper. It is possible that the formation of oxygen-hydrogen bonds contributes to this preservation. If the oxygen-hydrogen bonds form on the graphene/Cu surface, between the carbon atoms of the graphene, that could prevent the oxygen atoms from escaping during the anneal.

Evidence for oxygen intercalation can also appear in C 1s spectra¹⁸. Figure 2(b) clearly shows a drastic reduction in the number of observed peaks in the range of 286-291 eV, as well as shifted binding energies of the peak centered at approximately 284.5 eV. The intensities of the auxiliary peaks between 286-291 eV vary between the control and hydrogenated samples, but appear at roughly the same binding energies, which suggests that these peaks correspond to adsorbed residue on the surface. All peaks in the 286-291 eV range disappear after the hydrogenation and the control. Figure 2(c) displays a zoomed-in view of the spectra in Figure 2(b), excluding the auxiliary peaks. Before the hydrogenation and control, the graphene/Cu samples have their largest C 1s peak centered at 284.4 eV, which is the accepted binding energy for graphene^{18,19}. After the hydrogenation and control, the largest C 1s peak shifts to a binding energy of 284.6 eV. A binding energy of 284.75 eV has been proposed for graphene/Cu without any intercalated oxygen, while the standard 284.4 eV binding energy of graphene has been proposed to account for the presence of intercalated oxygen between the graphene and copper¹⁸. The shift away from the 284.4 eV binding energy of graphene/Cu with intercalated oxygen seems to be consistent with an interpretation of the O 1s spectra as showing decreased copper oxide formation after the hydrogenation and control compared to the original graphene/Cu samples. The graphene is not completely “coupled” to the copper, as would be the case if no copper oxide were present, but it is not as “decoupled” as it was before the hydrogenation and control, when more copper oxide was present between the graphene and copper¹⁸.

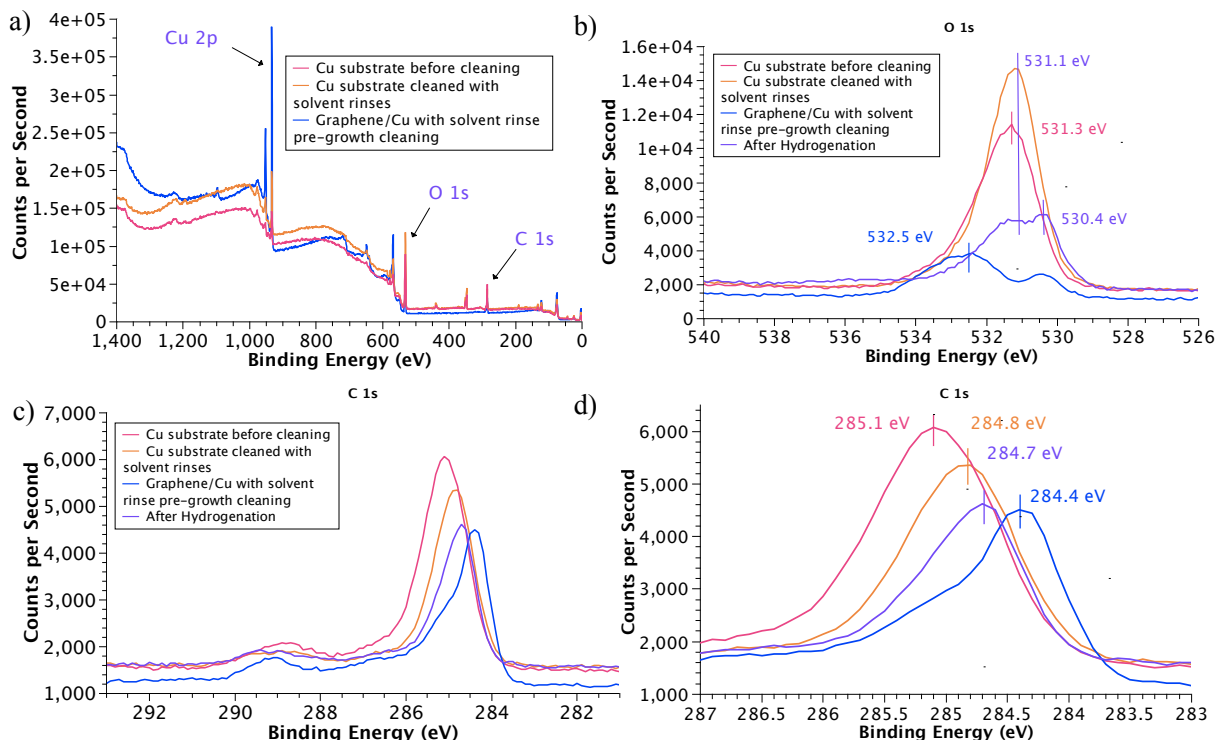
While the oxygen peak displays a clear difference between the hydrogenated and control spectra, the carbon peak is more difficult to decipher, as the hydrogenated and control peaks are very close in binding energy. The hydrogenated C 1s peak is slightly wider than that of the control peak, which could be due to a larger peak corresponding to carbon-hydrogen bonds. However, without a more careful analysis of how much the initial residue on the sample contributes to the profile of the C 1s spectrum, it is impossible to determine if additional widening of the peak could be due to hydrogenation.

To determine the effect of residue on the observed XPS profiles, XPS spectra of an unclean copper substrate and a clean copper substrate were compared with graphene/Cu spectra before and after hydrogenation. The copper foils used as growth substrates are cleaned with a solvent rinse chain of acetone, methanol, and isopropanol. The copper substrate of the graphene/Cu growth sample was cleaned with the solvent rinse chain before graphene growth. Figure 3(a) displays survey spectra from a copper foil before cleaning, a copper foil after cleaning, and a copper foil after graphene growth. The survey spectra reveal stark differences between the copper foils pre- and post-cleaning and the growth sample of graphene/Cu. The most noticeable difference is that the copper foil samples have broadened, curved regions in the range of 1400-1000 eV and 900-600 eV. In addition, the copper 2p peaks are suppressed compared to the sharp, intense copper 2p peaks of the growth sample. The broadened spectra and the weak intensities of the copper 2p peaks indicate that many electrons are inelastically scattered from the copper foil samples due to a significant amount of residue on the sample surface. The copper 2p electrons cannot escape easily because there are many other compounds on the surface of the sample, therefore the copper 2p and other elemental peak intensities are

suppressed. Before graphene growth, a significant amount of residue exists on the copper surface.

Comparing the spectra of the clean and unclean copper foils reveals few differences; the line profiles of the spectra and their overall intensities are similar. The lack of differences

Figure 3: Determining the Contribution of Residue to Graphene XPS Peaks



a) XPS Spectra of a copper foil substrate before cleaning, a copper foil substrate after cleaning, and a growth sample with graphene grown on copper foil. The cleaning process involved a solvent rinse chain of acetone, methanol, and isopropanol. The graphene/Cu growth sample was cleaned with the solvent rinse chain prior to graphene growth. b) and c) are XPS oxygen 1s spectra and carbon 1s spectra, respectively, of the copper foil substrate before cleaning, the copper foil substrate after cleaning, the graphene/Cu growth sample, and a graphene/Cu sample after being subjected to hydrogenation. d) Zoomed-in view of the largest peak in the C 1s spectrum. The center of each peak is marked with its corresponding energy.

between the two spectra indicates that the solvent rinse cleaning method does not rid the copper substrate of most of its inherent residue. Once the copper substrate is exposed to graphene growth, most of the residue in the ranges of 1400-1000 eV and 900-600 eV is removed. In these regions, the graphene/Cu growth sample spectrum displays profiles that are more linear instead of curved, and specific elemental peaks can be easily distinguished. In addition, the copper 2p

intensity is much more intense, which is expected as most of the sample is comprised of the bulk copper substrate. Although the growth process seems to clear a significant amount of the residue off the sample surface, for this experiment the amount of carbon and oxygen residue left on the sample surface was of particular interest.

The oxygen 1s spectra display dramatic changes in their profiles and intensities. Figure 3(b) shows the oxygen 1s spectra of an unclean copper foil, a clean copper foil, a graphene/Cu growth sample before hydrogenation, and a graphene/Cu growth sample after being subjected to hydrogenation. The growth sample and the hydrogenated sample spectra are not normalized so that their spectral profiles can be qualitatively compared with those of the clean and unclean copper foils. Due to the amount of residue on the surface of the pre-growth copper foils, the copper 2p intensities are not accurately displayed and cannot be used to normalize the other peaks in those spectra. The copper foil spectra pre- and post- cleaning display single, broad peaks centered at approximately 531 eV, which are likely composed of oxygen-hydrogen bonds as well as copper oxide and organic residue. The spectra before and after hydrogenation, while from a different hydrogenation sample than the data displayed in Figure 2, display the same trends as seen in the O 1s spectra in Figure 2(a); a copper oxide peak and a peak at 531 eV are observed after the hydrogenation.

Measuring a change in the carbon-hydrogen peak in the carbon 1s spectrum due to hydrogenation is already subtle enough to be challenging. Therefore it is important to try to minimize the amount of carbon residue left on the sample surface after graphene growth. With extra peaks in the C1s spectrum corresponding to various forms of carbon residue, it is difficult to isolate the small peak corresponding to carbon-hydrogen bonds and determine changes due to hydrogenation. Figure 3(c) shows the carbon 1s spectra of an unclean copper foil, a clean copper

foil, a graphene/Cu growth sample, and a graphene/Cu growth sample after being subjected to hydrogenation. Once again, the growth and hydrogenation sample spectra are not normalized for the purpose of qualitative comparison with the copper foil spectra.

The carbon 1s spectra display few obvious deviations from the spectrum of the unclean copper foil. As is seen in Figure 3(c), the spectral profiles of all four samples are very similar, and the satellite peak at approximately 289 eV is present in each sample, indicating that this peak corresponds to some residue inherent on the copper foil source. The larger, more intense peak in the spectrum at approximately 285 eV is observed to shift in energy. However, it must be noted that since the profiles of the four samples are extremely similar, it is very difficult to distinguish how much of the carbon 1s peak corresponds to graphene, hydrogenated graphene, and leftover residue on the graphene/Cu surface. Raman spectra of the growth sample and hydrogenated sample confirm that each sample contains graphene, so a graphene signature in the XPS spectra is expected, but its intensity relative to other peaks of carbon-containing compounds cannot be explicitly determined.

Upon closer inspection of the spectra, the hydrogenated sample again shows a shift in binding energy from 284.4 eV to 284.7 eV, as displayed in Figure 3(d). This shift, as discussed previously, is consistent with the graphene shifting from being “decoupled” with an intercalated oxygen layer to being more closely “coupled” to the copper with less intercalated oxygen¹⁸. To emphasize the difficulty in determining whether the sample subjected to hydrogenation is actually hydrogenated, a C1s spectrum of a sample after hydrogenation was fitted with several peaks accounting for the presence of some coupled graphene, decoupled graphene, defects, and sp³ hybridized carbon. The fit is displayed in Figure 4(a) and compared to the curve fit in the literature from which it was inspired, shown in Figure 4(b). The peak at 285.2 eV is commonly

attributed to sp^3 -hybridized carbon¹⁸. The peak at 288.6 eV is attributed to residue on the graphene. Slight changes in the intensity of the 285.2 eV peak are used to determine whether a sample is hydrogenated¹⁹, however without carefully accounting for any residue left over on the sample, it is difficult to accurately interpret changes in the intensity due to hydrogenation. As

Figure 4: Comparison of Hydrogenated Sample Curve Fit with Pristine Graphene/Cu Curve Fit

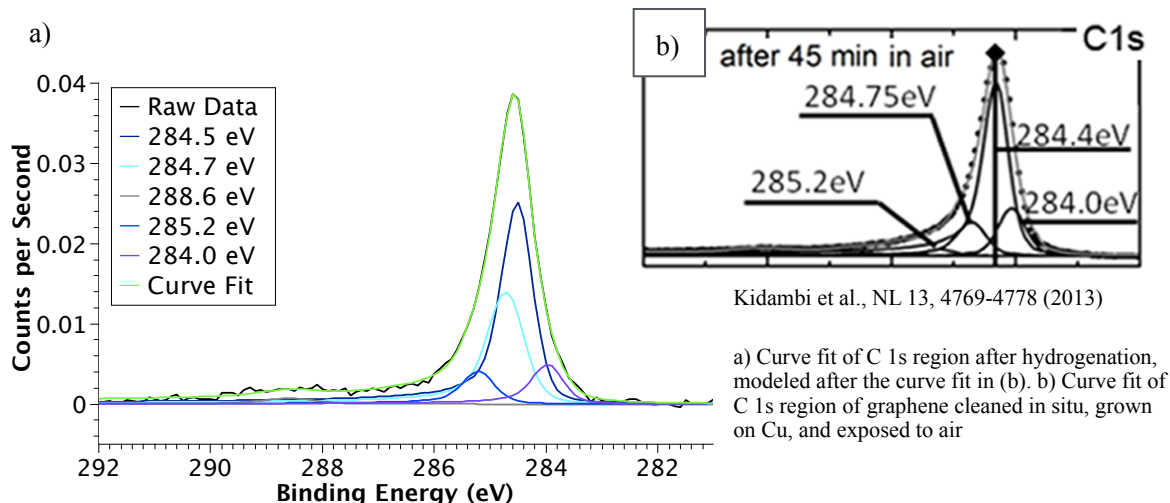


Figure 4(b) shows, even pristine graphene/Cu has a native 285.2 eV peak corresponding to sp^3 -hybridized carbon. Therefore studying the XPS spectra obtained in this experiment does not clearly determine whether the graphene is hydrogenated or not. The graphene may be hydrogenated, but hydrogenation cannot be confirmed without further experiments to minimize the amount of residue initially on the graphene/Cu surface.

V. Conclusion

This work shows that graphene on copper does not appear to have any additional defects after being annealed in vacuum, and the hydrogenation procedure may preserve some of the initial intercalated oxygen between the graphene and copper. While the Raman and XPS data do

not conclusively determine whether or not the samples subjected to hydrogenation are actually hydrogenated, this study of spectral features contributes to a greater understanding of the interaction between graphene, its substrate and its adsorbates, which is crucial for further elucidating differences in the spectra corresponding to hydrogenation. Future work will involve determining if the presence of hydrogen in the chamber does somehow prevent the intercalated oxygen from escaping during the anneal, and if the remaining presence of copper oxide is dependent on the specific gas introduced into the chamber. In addition, an in-situ Raman spectroscopy system is currently in development and could be used to determine if the presence or absence of intercalated oxygen between the graphene and copper is reflected in the graphene Raman spectrum. While many details still have yet to be discovered about graphene's interaction with the copper substrate and intercalated oxygen, this work shows that these interactions may become important when creating hydrogenated graphene.

VI. Acknowledgements

I would like to thank Dr. Jay Gupta for the significant amount of time and effort he spent advising me, and for giving me the opportunity to do this project. I would also like to thank Shawna Hollen for her advice and encouragement throughout the course of this project. Grady Gambrel, Steven Tjung, Josh Schulter, and Anne Benjamin have each helped me during this project, which I greatly appreciate. I also want to thank Lisa Hommel for helping me take the XPS data and get started on learning how to analyze it. Finally, I would like to thank Sara Mueller and all of the students in the Graphene Factory for their hard work in producing high-quality graphene.

VII. References

- [1] Johns, James E. and Hersam, Mark C. "Atomic Covalent Functionalization of Graphene." *Accounts of Chemical Research*. 46.1 (2013): 77-86.
- [2] Elias, D.C. et al. "Control of Graphene's Properties by Reversible Hydrogenation: Evidence for Graphane." *Science*. 323. (2009): 610-3.
- [3] Ferrari, A. and Basko, D. "Raman Spectroscopy as a Versatile Tool for Studying the Properties of Graphene." *Nature Nanotechnology*. 8.4 (2013): 235-246.
- [4] Pumera, M. and Wong, C. "Graphane and Hydrogenated Graphene." *Chemical Society Reviews*. 42. (2013): 5987-5995.
- [5] Ferrari, A. et al. "Raman Spectrum of Graphene and Graphene Layers." *Physical Review Letters*. 97.18. (2006): 187401-1-4.
- [6] Yu, Q. et al. "Control and Characterization of Individual Grains and Grain Boundaries in Graphene Grown by Chemical Vapour Deposition." *Nature Materials*. 10.6. (2011): 443-449.
- [7] Mattevi, C. et al. "A Review of Chemical Vapour Deposition of Graphene on Copper." *Journal of Materials Chemistry*. 21.10. (2011): 3324-3334.
- [8] Suk, J. "Transfer of CVD-Grown Monolayer Graphene Onto Arbitrary Substrates." *ACS Nano*. 5.9. (2011): 6916-6924.
- [9] Zhou, C. et al. "Graphene's Cousin: the Present and Future of Graphane." *Nanoscale Research Letters*. 9. (2014): 26-35.
- [10] Georgakilas, V. et al. "Functionalization of Graphene: Covalent and Non-Covalent Approaches, Derivatives, and Applications." *Chemical Reviews*. 112. (2012): 6156-6214.
- [11] Roe, M. *Surface Characterization of Hydrogenated CVD Diamond*. Undergraduate Thesis. The Ohio State University, 2010.
- [12] Fadley, C.S. "Basic Concepts of X-ray Photoelectron Spectroscopy." *Electron Spectroscopy: Theory, Techniques, and Applications*. London: Academic Press, 1978.
- [13] Hong, J. et al. "Origin of New Broad Raman D and G Peaks in Annealed Graphene." *Scientific Reports*. 3. (2013): 2700.
- [14] Malard, L. M. et al. "Raman Spectroscopy in Graphene." *Physics Reports*. 473.5-6. (2009): 51-87.

- [15] Lucchese, M. et al. "Quantifying Ion-Induced Defects and Raman Relaxation Length in Graphene." *Carbon*. 48.5. (2010): 1592-1597.
- [16] Lin, Y. et al. "Clean Transfer of Graphene for Isolation and Suspension." *ACS Nano*. 5.3 (2011): 2362-2368.
- [17] Casiraghi, C. et al. "Raman Fingerprint of Charged Impurities in Graphene." *Applied Physics Letters*. 91. (2007): 233108-1-3.
- [18] Kidambi, P. et al. "Observing Graphene Growth: Catalyst-Graphene Interactions During Scalable Graphene Growth on Polycrystalline Copper." *Nano Letters*. 13. (2013): 4769-4778.
- [19] Jayasingha, R. et al. "In Situ Study of Hydrogenation of Graphene and New Phases of Localization between Metal-Insulator Transitions." *Nano Letters*. 13. (2013): 5098-5105.